

Mechanical Design Concept of Superconducting Magnet System for Helical Fusion Reactor

journal or publication title	Fusion Science and Technology
volume	75
number	5
page range	384-390
year	2019-04-30
NAIS	11900
URL	http://hdl.handle.net/10655/00012723

doi: 10.1080/15361055.2019.1603041



Mechanical design concept of superconducting magnet system for helical fusion reactor

Hitoshi Tamura¹, Nagato Yanagi¹, Takuya Goto¹, Junichi Miyazawa¹, Teruya Tanaka¹, Akio Sagara¹, Satoshi Ito², Hidetoshi Hashizume²

¹National Institute for Fusion Science, Toki, Japan

²Tohoku University, Sendai, Japan

Corresponding author: Hitoshi Tamura

Email: tamura@nifs.ac.jp

Abstract:

The conceptual design of a helical fusion reactor was studied at the National Institute for Fusion Science in collaboration with other universities. FFHR-d1 is a self-ignition demonstration reactor that operates with a major radius of 15.6 m at a magnetic field intensity of 4.7 T. FFHR-c1 is a compact sub-ignition reactor that aims to realize steady electrical self-sufficiency. Compared to FFHR-d1, FFHR-c1 has a magnetic field intensity of 7.3 T and a geometrical scale of 0.7. The location of the superconducting coils in both types of FFHR is based on that of the Large Helical Device (LHD). LHD has a major radius of 3.9 m. According to the design of LHD, the deformation must be within the required value to compensate for the accuracy of the magnetic field. According to this concept, the magnet support structure of the LHD was fabricated using thick stainless steel 316 to impart sufficient rigidity. Thus, the stress of the magnet system of LHD is sufficiently below the permissible stress. In the case of FFHR, from the viewpoint of the reactor, a large access port is required for the maintenance of the in-vessel components. Mechanical design of the support structure is conceptualized by considering the basic thickness of the material and residual aperture space by referencing the mechanical analysis results. Details of the design concepts of LHD and FFHR-d1/c1, as well as the results of mechanical analyses, are introduced in this paper.

Keywords:

Helical fusion reactor, FFHR, Large helical device, Superconducting magnet, Structural analysis

I. Introduction

Helical fusion reactors have attractive features, such as steady-state operation in the absence of a plasma current drive and a built-in helical diverter. These features favor their use as practical fusion power plants. The National Institute for Fusion Science is developing a conceptual design of the Large Helical Device (LHD) [1]- type helical reactor, FFHR [2, 3]. Research and development of reactor components is being conducted in collaboration with various Japanese universities. FFHR is the abbreviated form of Force Free Helical Reactor. The original concept was based on force-free-like configuration of helical coils (HCs) to reduce electromagnetic (EM) force. [Figure 1](#) shows the development history of the FFHR series of reactors. A design study was started with FFHR1, which had three HCs ($l = 3$). Then, the concept was revised several times to reduce size (FFHR2), ensure a blanket space, and increase the coil major radius and decrease the stored magnetic energy by reducing the magnetic field (FFHR2m1), and achieve a coil geometry similar to that of LHD (FFHR2m2). Considering the optimized blanket space and the radial build between the plasma and the helical coil, FFHR-d1 was established as a self-ignition commercial reactor. FFHR-d1 has a major radius of 15.6 m, and it generates a magnetic field intensity of 4.7 T at the magnetic center. By contrast, FFHR-c1 is a design for a compact sub-ignition reactor that aims to realize steady electrical self-sufficiency. FFHR-c1 has a magnetic field intensity of 7.3 T, and its scale is 0.7 that of FFHR-d1. The geometries of the magnet systems for both types of FFHR, including a pair of HCs and two sets of vertical field coils (VFCs), are based on the geometry of LHD. LHD has a major radius of 3.9 m and magnetic field intensity of 4 T (in design with 1.8 K superfluid helium cooling: actual achievement is 3 T with 4 K liquid helium). [Figure 2](#) shows schematics and specifications of LHD, FFHR-d1, and FFHR-c1.

The accuracy of the coil winding section is one of the most important issues for a magnet-confinement-type fusion reactor. Moreover, soundness of the structure must be guaranteed.

Therefore, the mechanical design must consider not only stress distribution but also displacement behavior. The fundamental shape and structural material selection can be decided according to such conception with various design conditions.

The design conception for LHD and FFHR-d1/c1, as well as the results of EM and mechanical analyses, are presented in this paper. Weight estimation with the virial theorem and prospects for future fusion reactors are discussed as well.

II. Structural design conception

II.A. LHD

The construction of LHD was completed in 1997, and the plasma experiment with hydrogen was started in 1998. A new experimental campaign that uses deuterium has started since 2017 [4]. The accuracy of the coil winding section was set to 2 mm during construction and to 3.4 mm against deformation due to EM force under 4 T operation in the design phase of LHD, so the error field ratio at the plasma center is $<1 \times 10^{-4}$ [5]. Therefore, in the mechanical design, the priority was to ensure that the deformation remains within the required value. According to this conception, the magnet support structure of LHD was designed and fabricated using 100-mm-thick stainless steel (SS) 316 achieving adequate rigidity. Analytical results showed that the maximum Tresca stress of 290 MPa and the maximum deformation of 2.62 mm appeared under normal coil excitation [6]. The permissible stress of SS 316 used for LHD is approximately 630 MPa at 4 K. Thus, the stress of the magnet system of LHD is adequately lower than the permissible stress.

II.B. FFHR-d1

In the case of FFHR, from the viewpoint of practical fusion reactors, a large access port is required for maintaining the in-vessel components, such as tritium breeding blanket, neutron shielding blanket, and diverter, because these components must be replaced periodically. The helical-type reactor has wide aperture between a pair of HCs, but a tough structure is needed to sustain the huge magnetic energy of more than 100 GJ, and the available space decreases as the volume of the coil support structure increases. Achieving large apertures and adequate strength were the priorities in the structural design of the magnet system of FFHR. Mechanical design of

the support structure was conceptualized by considering the basic thickness of the material and residual aperture space by referencing the mechanical analysis results. EM force and stress analysis were conducted to investigate the optimal design suited for the helical reactor. Design modification in terms of aperture size, additional ribs, and corner fillet was repeated until the maximum stress was within the allowable level.

II.B.1. EM force

To determine the magnetic field distribution and EM force, coil geometry and cross-sectional shape were defined. The coil winding consists of 390 turns of superconductor. The superconductor has a square shape, with each side measuring 62 mm, including the insulating material. The operating current of the superconductor is 102 kA in the case of FFHR-d1 with an additional helical coil (named NITA coil [7, 8]), that is, the overall magneto-motive force is 39.7 MA, and the current density is 26.5 A/mm². The two sets of VFCs are assumed to have rectangular cross-sections. The magnetic field distribution was calculated with the finite element method by using vector potential elements in ANSYS. [Figure 3](#) shows the results of the magnetic field and EM force vector distributions at every single superconductor on the inboard side of the torus. The magnetic field along the lateral direction induces hoop force and that along the minor radius direction induces overturning force on the coil. The calculated maximum overall EM hoop force F_a and the overturning force F_b in each cross-section of the HC were 69 and ± 8 MN/m, respectively, as shown in [Fig. 4 \[9\]](#).

II.B.2. Superconductor and structural material

There are several candidate superconductors for the HC winding, including forced flow with a cable-in-conduit conductor (CICC) by using a low-temperature superconductor (LTS) [10], indirect cooling with an LTS [11], and helium gas cooling with a high-temperature superconductor (HTS) [12]. Figure 5 shows the schematics of each candidate superconductor. Candidates for use as the LTS are Nb₃Sn and Nb₃Al with 4 K helium cooling as the estimated maximum magnetic field is 12 T. The 100 kA class LTS for FFHR-d1 can be available by advancing the 68 kA conductor developed for the ITER TF coil. Rare-earth barium copper oxide (REBCO) coated conductor is a candidate as the HTS and higher operating temperature, e.g. 20 K is expected. Although the current capacity is based on a recent commercial REBCO coated conductor, higher current capacity and reduction of anisotropy against the magnetic field direction are desirable to achieve the high overall current density and to cope with the complex 3-dimensional magnetic field distribution of the helical coil system. Liquid hydrogen is an alternative candidate coolant for the HTS. The cooling scheme should be carefully chosen considering electrical/thermal issues such as stability, quench protection, heat transfer, heat capacity, circulation pump power, etc. Physical properties of the superconductors were calculated by performing multi-scale homogenization analysis. Table 1 lists the obtained physical properties, which were used for the structural analyses [13].

Non-magnetic SS can be a candidate structural material for the coil support structure. More than 250-mm-thick SS 316LN with a yield strength of >900 MPa has been developed under the ITER project. Moreover, 260-mm-thick welding has been demonstrated using this material [14].

Presently, it is a practical candidate for use as structural material in FFHR.

II.B.3 Stress analysis

For instance, when using the gas-cooled HTS for the coil winding and adopting SS 316LN with a typical thickness of 250 mm for the coil support structure, the maximum von Mises stress and deformation were found to be 764 MPa and 25 mm, respectively [9], as shown in Fig. 6.

Consequently, the stress level is within the permissible value, whereas the maximum deformation exceeds the LHD criterion. The deformation can be reduced by increasing the typical thickness; however, doing so may affect material manufacturing and welding feasibility. Further structural optimization will be needed if the deformation is not acceptable from the viewpoint of the plasma confinement investigation.

Multi-scale analysis helps obtain both the stress in the support structure and the local stress in the superconductor. The nominal strain along the coil winding was lower than 0.16%, which is adequately low against the strength of HTS material. By contrast, the shear stress in the HTS was 35 MPa, as shown in Fig. 7. The analytical results were used to select the insulating material and set the criterion for joint strength between HTS conductors [15].

II.C. FFHR-c1

II.C.1. Scaling from FFHR-d1

The positional relationships among the superconducting coils are similar in FFHR-d1 and c1.

This relationship is similar to that of the LHD coil configuration, except that LHD has three sets of VFCs while FFHR has two sets of VFCs. The magnetic field intensity of FFHR-c1 is (7.3/4.7) times larger than that of FFHR-d1, and its scale is 0.7 that of FFHR-d1. Generally, EM force and stress intensity yield the following scaling law:

When dimensions are proportional to device size R (e.g., major radius) under magnetic field intensity B ,

magneto-motive force $I [A] \propto R \times B$,

EM force $F [N/m] \propto B \times I \propto R \times B^2$,

stress $\sigma [N/m^2] \propto F \times R / R^2 \propto B^2$.

Stress does not depend on size but is proportional to the square of magnetic field intensity.

Moreover, if the cross-sectional area of the coil is similar to each other,

current density $j [A/m^2] \propto B / R$.

Direct scaling from FFHR-d1 to FFHR-c1 results in a 2.4-fold increase in stress and a 2.2-fold increase in current density, that is, the maximum von Mises stress increases from 764 MPa to 1.8 GPa, and the current density of HC increases from 26.5 A/mm² to 58.8 A/mm². The stress is excessive, and the high current density is undesirable from the standpoint of quench protection. It is necessary to redesign the structure in consideration of the coil cross-section, thickness, aperture size, etc.

II.C.2. Modifications of coil and support structure

Based on the coil geometry of FFHR-d1, the fundamental layout of the coils and the support structure for FFHR-c1 were modeled. During the design modification, the cross-sectional shape of the HC was selected carefully to ensure appropriate clearance between the HC and the blanket system. The superconductor used in the FFHR-c1 was assumed to have a structure similar to that of d1, and the size was reduced to 43.32 mm × 43.32 mm to achieve the current density of 47.7 A/mm², as decided based on the results of a hot spot quench analysis. The magneto-motive force of the HC is 45.99 MA. By using these specifications, the magnetic field distribution and the EM force were calculated. The maximum EM hoop force F_a was found to be 119 MN/m, and the maximum EM overturning force F_b was found to be approximately ±30 MN/m.

In the structural analysis of FFHR-c1, a gas-cooled HTS with REBCO coated superconductor was adopted since the maximum magnetic field on the coil was estimated to reach 19 T, and to be able to operate at high temperatures. The support structure was assumed to be made of SS 316LN with a basic thickness of 200 mm. The design was rearranged until the maximum von Mises stress in the structure decreased to an acceptable level, especially in stress concentration areas, such as corner regions of apertures. [Figure 8](#) shows the results of the structural analysis. The maximum von Mises stress appears on the outer port corner as the peak stress. Spatial stress distribution does not exceed 790 MPa. The soundness of the support structure will be guaranteed if a high-strength material is used. The maximum deformation is approximately 16 mm, and it appears in the outer VFC region.

III. Weight estimation

The weights of the support structures in the latest design of FFHR-d1 and c1 are 22,000 tons and 11,000 tons, respectively. According to the virial theorem, which states that the total weight of the coil support is proportional to the stored magnetic energy [\[16\]](#), that is,

$$M = Q\rho E / \sigma, \quad (1)$$

where M is total weight, ρ is density of structural material, E is stored magnetic energy, σ is allowable stress, and Q is a correction factor (~ 3). As shown in [Fig. 9](#), existing devices are considerably heavier than the estimates made using the virial theorem. The total weight of FFHR-c1 is close to the range of the estimated weight, with a stored magnetic energy of 160 GJ, which is between 10,000 (theoretical) and 30,000 tons. Weight reduction can be achieved by optimizing the design of the support structure. Although FFHR-d1 and c1 store almost the same amount of magnetic energy, the total weight of c1 is considerably lower than that of d1. Required

amount of structural material depends on the maximum stress criteria, of course, and further reduction can be achieved because low-stress regions exist in the structure. A novel design method, for example, topology optimization, can be employed to possibly solve this issue. By contrast, if weight reduction is given priority, deformation will increase inevitably. The deformation effect on plasma confinement must be confirmed and adjusted simultaneously. The accuracy of the magnetic field can be compensated by structural design (e.g. using pre-deformed shape) or using additional correction coils, etc.

V. Summary

EM-mechanical analysis is a crucial issue for helical fusion reactors. Design conceptions and the results of structural analyses of LHD and FFHR-d1/c1 were presented herein. The LHD design prioritizes magnetic field accuracy because it is a plasma physics experimental device. For that reason, minimum deformation was the first criterion in its design. By contrast, because FFHR is a commercial/demonstration reactor, a large aperture size under certain allowable stress is prioritized in its design. Fusion reactor is estimated to need tens of thousands tons of structural material. The virial theorem suggests the possibility of weight reduction, but such a reduction may lead to an increase in deformation. Accuracy compensation should be considered together with core plasma investigations.

Acknowledgments

The present study has been conducted under the grant from the NIFS (No. UFFF031). This work was supported by JSPS KAKENHI Grant Numbers 26220913, 16K06943, and 17H03507.

References

- [1] O. MOTOJIMA et al., “Physics and engineering design studies on the Large Helical Device,” *Fus. Eng. Des.*, **20**, 3 (1993); [https://doi.org/10.1016/0920-3796\(93\)90019-E](https://doi.org/10.1016/0920-3796(93)90019-E).
- [2] A. SAGARA et al., “Review of stellarator/heliotron design issues towards MFE DEMO,” *Fus. Eng. Des.*, **85**, 1336 (2010); <https://doi.org/10.1016/j.fusengdes.2010.03.041>.
- [3] A. SAGARA et al., “Design activities on helical DEMO reactor FFHR-d1,” *Fus. Eng. Des.*, **87**, 594 (2012); <https://doi.org/10.1016/j.fusengdes.2012.01.030>.
- [4] Y. TAKEIRI et al., “Extension of the operational regime of the LHD towards a deuterium experiment,” *Nucl. Fus.*, **57**, 102023 (2017); <https://doi.org/10.1088/1741-4326/aa7fc2>.
- [5] K. YAMAZAKI et al., “Requirement for accuracy of superconducting coils in the Large Helical Device,” *Fus. Eng. Des.*, **20**, 79 (1993); [https://doi.org/10.1016/0920-3796\(93\)90027-F](https://doi.org/10.1016/0920-3796(93)90027-F).
- [6] A. NISHIMURA, S. IMAGAWA, and H. TAMURA, “Cryogenic structural material and design of support structure,” *Journal of Cryogenic Society of Japan*, **32 (11)**, 48 (1997) (in Japanese); <https://doi.org/10.2221/jcsj.32.586>.
- [7] N. YANAGI et al., “NITA coil — innovation for enlarging the blanket space in the helical fusion reactor,” *Plasma Fus. Res.* **11**, 2405034 (2016); <https://doi.org/10.1585/pfr.11.2405034>.
- [8] N. YANAGI et al., “Progress in the Conceptual Design of the Helical Fusion Reactor FFHR-d1,” *J. Fus. Energ.* (2018); <https://doi.org/10.1007/s10894-018-0193-y>.

- [9] H. TAMURA et al., "Design modification of structural components for the helical fusion reactor FFHR-d1 with challenging options," *Fus. Eng. Des.*, **124**, 605 (2017);
<https://doi.org/10.1016/j.fusengdes.2017.03.031>.
- [10] S. IMAGAWA et al., "Concept of magnet system for LHD-type reactor," *Nucl. Fus.* **49**, 075017 (2009); <https://doi.org/10.1088/0029-5515/49/7/075017>.
- [11] K. TAKAHATA et al., "A cooling concept for indirectly cooled superconducting magnet for the fusion reactor FFHR," *Plasma Fus. Res.* **10**, 3405011 (2015);
<https://doi.org/10.1585/pfr.10.3405011>.
- [12] N. YANAGI et al., "Design and development of high-temperature superconducting magnet system with joint-winding for the helical fusion reactor," *Nucl. Fus.* **55**, 053021 (2015);
<https://doi.org/10.1088/0029-5515/55/5/053021>.
- [13] H. TAMURA et al., "Multiscale stress analysis and 3D fitting structure of superconducting coils for the helical fusion reactor," *IEEE Trans. Appl. Supercond.* **26** (3), 4202405 (2016);
<https://doi.org/10.1109/TASC.2016.2531008>.
- [14] Y. CHIDA et al., "Validation of welding technology for ITER TF coil structure," *Fus. Eng. Des.*, **86**, 2900 (2011); <https://doi.org/10.1016/j.fusengdes.2011.06.004>.
- [15] S. ITO et al., "Fundamental Investigation on Tensile Characteristics of a Mechanical Lap Joint of REBCO Tapes," *IEEE Trans. Appl. Supercond.* **25** (3), 4201205 (2015);
<https://doi.org/10.1109/TASC.2014.2369058>
- [16] K. TAKAHATA, "Superconducting coils for fusion," *Journal of Plasma and Fusion Research* 81 (4), 273 (2006) (in Japanese);
http://www.jspf.or.jp/Journal/PDF_JSPF/jspf2005_04/jspf2005_04-272.pdf.

Table

Table I
Homogenized equivalent physical properties of the superconductors

	Gas-cooled HTS	CICC LTS	Indirect- cooled LTS
E_x (GPa)	79.6	121.3	114.0
E_y (GPa)	79.4	121.3	103.1
E_z (GPa)	156.1	144.9	114.0
G_{xy} (GPa)	44.6	39.8	37.4
G_{yz} (GPa)	43.9	47.7	37.5
G_{xz} (GPa)	44.0	47.7	43.6
ν_{xy}	0.394	0.279	0.314
ν_{yz}	0.149	0.244	0.283
ν_{xz}	0.150	0.244	0.308

E_i is Young's modulus in the i -direction, ν_{ij} is Poisson's ratio for a transverse strain in the j -direction when stressed in the i -direction, and G_{ij} is the shear modulus in the i - j plane. The local coordinate x, y, z represent height, width, and longitudinal direction of each conductor, respectively.

Figure captions

Figure 1 Development history of FFHR series [2].

Figure 2 Schematics of LHD, FFHR-d1, and FFHR-c1.

Figure 3 Magnetic field and EM distribution in HC at inboard side of the torus.

Figure 4 Overall EM force on the HC of FFHR-d1 [9].

Figure 5 Cross-section of the candidate superconductor for FFHR-d1 [13].

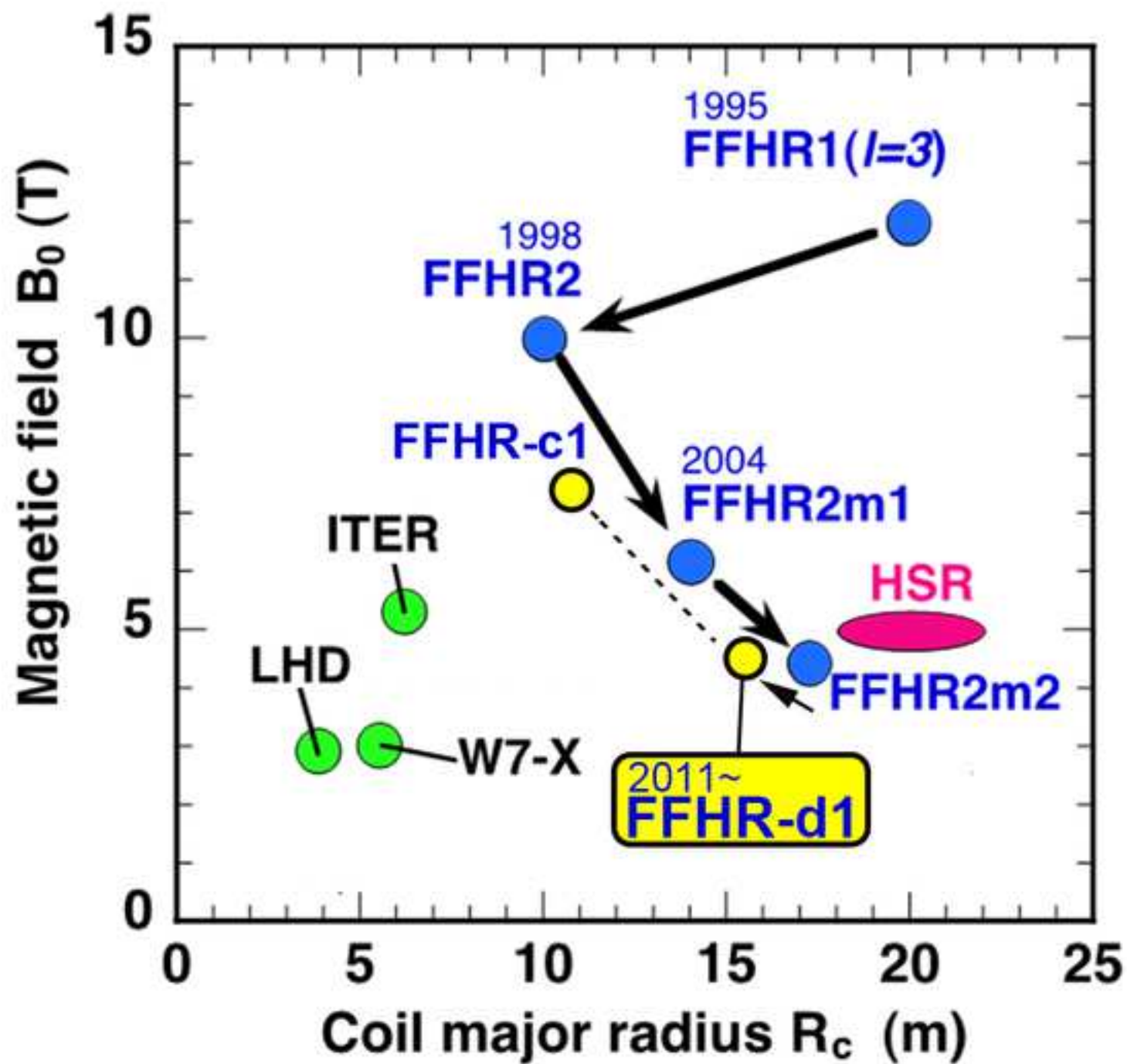
Figure 6 Von Mises stress distribution in the coil support structure [9].

Figure 7 Shear stress distribution in the HC and in the HTS region of the superconductor [9].

Figure 8 Von Mises stress distribution of the support structure of FFHR-c1.

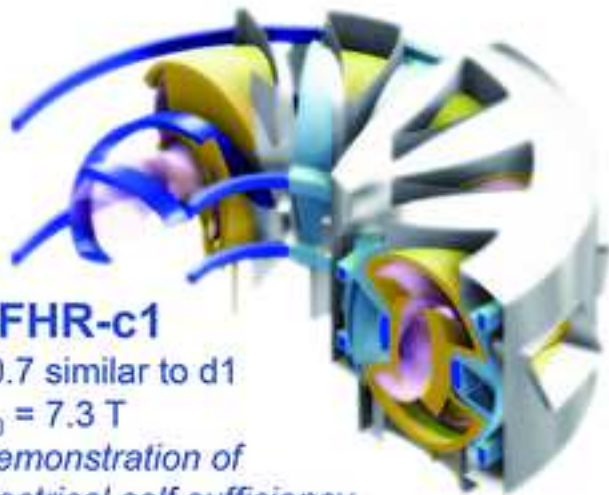
Figure 9 Total weight of magnet system in fusion devices as a function of a magnetic stored energy [16].

Figs 6, 7, and 8; original color drawings for the online version, and black-white/gray scale drawings for the print version are both enclosed.

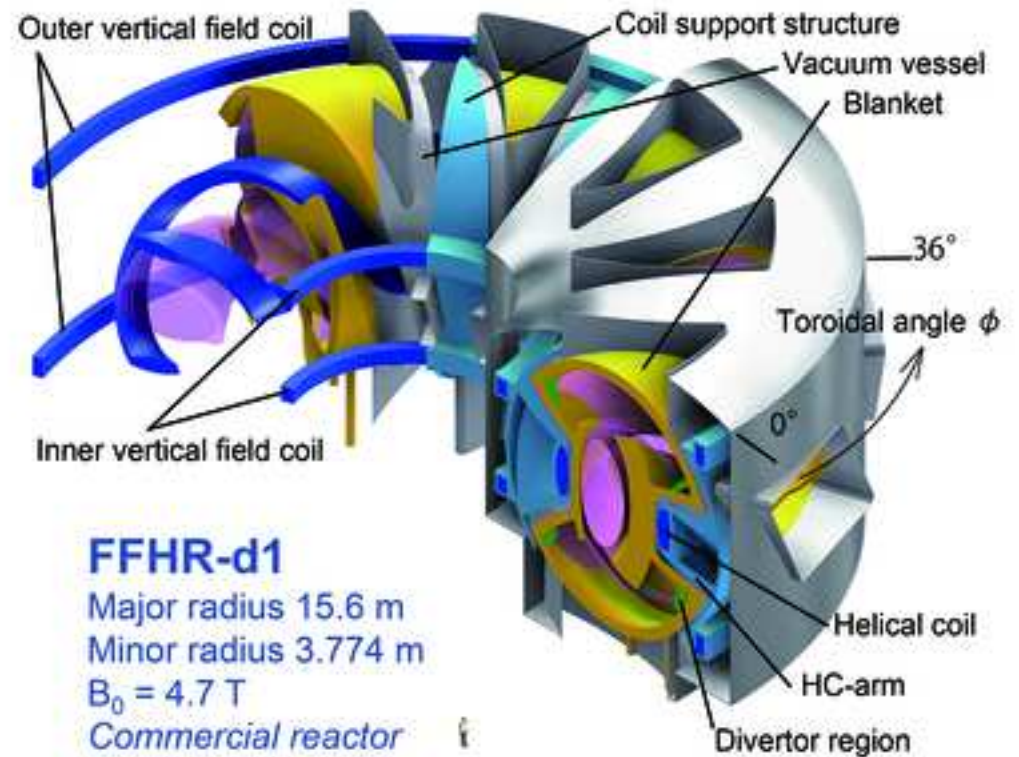


LHD

Major radius 3.9 m
 Minor radius 0.975 m
 $B_0 = 4$ T (in design)
Plasma experiment

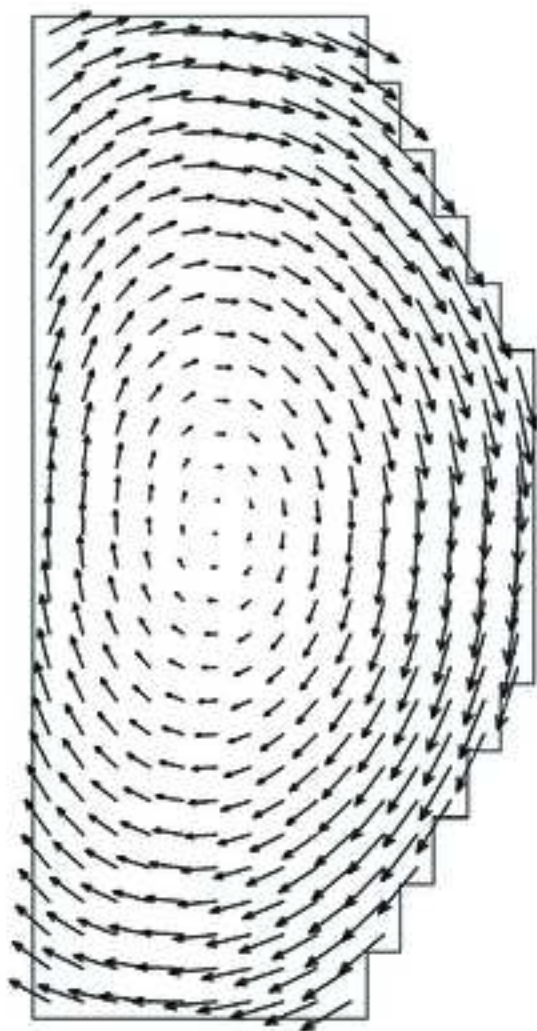
**FFHR-c1**

x0.7 similar to d1
 $B_0 = 7.3$ T
Demonstration of electrical self sufficiency

**FFHR-d1**

Major radius 15.6 m
 Minor radius 3.774 m
 $B_0 = 4.7$ T
Commercial reactor

Magnetic field vector map



EM force vector map

